



## Original article

# Design, synthesis, biological evaluation and molecular modeling studies of 1-aryl-6-(3,4,5-trimethoxyphenyl)-3(Z)-hexen-1,5-diyne as a new class of potent antitumor agents

Yu-Hsiang Lo<sup>a,1</sup>, Ying-Ting Lin<sup>c,1</sup>, Yu-Peng Liu<sup>d</sup>, Tsai-Hui Duh<sup>e</sup>, Pei-Jung Lu<sup>d,\*\*</sup>, Ming-Jung Wu<sup>b,e,\*</sup>

<sup>a</sup> Graduate Institute of Pharmaceutical Science, Kaohsiung Medical University, Kaohsiung, Taiwan

<sup>b</sup> Department of Chemistry, National Sun Yat-sen University, Kaohsiung, Taiwan

<sup>c</sup> Department of Biotechnology, Kaohsiung Medical University, Kaohsiung, Taiwan

<sup>d</sup> Institute of Clinical Medicine, National Cheng Kung University, Tainan, Taiwan

<sup>e</sup> Department of Medicinal and Applied Chemistry, Kaohsiung Medical University, Kaohsiung, Taiwan

## ARTICLE INFO

## Article history:

Received 29 November 2012

Received in revised form

1 January 2013

Accepted 8 January 2013

Available online 21 January 2013

## Keywords:

Enediyne

G2/M arrest

Apoptosis

Microtubule depolymerization

## ABSTRACT

A series of novel enediyne-containing molecules, 1-aryl-6-(3,4,5-trimethoxyphenyl)-3(Z)-hexen-1,5-diyne, were synthesized and displayed significant IC<sub>50</sub> values of 10<sup>-7</sup> to 10<sup>-6</sup> M against various cancer cell lines. Of these compounds, 1-(2-pyridinyl)-6-(3,4,5-trimethoxyphenyl)-3(Z)-hexen-1,5-diyne (**8**) demonstrated the greatest growth inhibition activity. Compound **8** also arrested cancer cells in the G2/M phase and induced apoptosis *via* activation of Caspase-3. In addition to the G2/M block, compound **8** caused microtubule depolymerization at low concentrations and markedly decreased tumor size in xenographic studies.

© 2013 Elsevier Masson SAS. All rights reserved.

## 1. Introduction

Microtubules are a component of the cytoskeleton formed by highly dynamic assemblies of tubulin heterodimers, including  $\alpha$ - and  $\beta$ -tubulins. Microtubules and their dynamics play a crucial role in many biological processes, including mitosis, intracellular transport, exocytosis and cell growth [1]. Because microtubules are important in mitosis and cell division, they have been targets for the development of a number of new anticancer drugs [2]. These drugs are often classified into two major groups: the microtubule-stabilizing agents (inhibit microtubule depolymerization) and the microtubule-destabilizing agents (enhance microtubule depolymerization) [3]. The microtubule-stabilizing agents bind in the taxoid binding site, such as taxol and docetaxel [4]. Most microtubule-destabilizing agents bind in the “vinca” binding site or the “colchicine” binding site, such as vinca alkaloids [5], colchicine [6], and combretastatin A-4 [7]. For instance, combretastatin A-4

(CA-4) shows potent inhibition of microtubule polymerization by blocking the colchicine binding site and rapidly shutting down existing tumor vasculature at doses below the maximum tolerated dose [8]. CA-4 may block cells in the G2/M phase of the cell cycle and induce apoptosis [9].

In our earlier publications [10], we reported a series of 1,6-diaryl-3(Z)-1,5-diyne as new antitumor agents. Of those compounds, 2-(6-(2-trifluoromethylphenyl))-3(Z)-(hexen-1,5-diyne) aniline (**1**) demonstrated the most potent cytotoxic activity against tumor cells at a concentration of 10<sup>-7</sup> M, inducing a massive accumulation of cells in G2/M phase and apoptosis *via* activation of the Caspase family [10c]. A brief exposure of MDA-MB-231/ATCC cells to compound **1** was sufficient to produce sustained depolymerization of the microtubules in a concentration-dependent manner. According to our ligand-docking experiment [11], compound **1** binds to  $\alpha$ - and  $\beta$ -tubulin in the same manner as colchicine. The amino group of compound **1** forms hydrogen bonds with the amino acids 179-Thr and 181-Val of  $\alpha$ -tubulin, as would the hydroxyl group of CA-4 and the carbonyl group of colchicine. The trifluoromethylphenyl group of compound **1** sits in the pocket of  $\beta$ -tubulin, similar to the trimethoxyphenyl subunits of colchicine and CA-4. Although several 1,6-diaryl-3(Z)-1,5-diyne with trimethoxyphenyl subunits have been reported by Provot [12], such as

\* Corresponding author. Department of Chemistry, National Sun Yat-sen University, Kaohsiung, Taiwan. Fax: +886 7 5253909.

\*\* Corresponding author.

E-mail address: [mijuwu@faculty.nsysu.edu.tw](mailto:mijuwu@faculty.nsysu.edu.tw) (M.-J. Wu).

<sup>1</sup> Equal contribution.

compounds **2a** and **2b** [12], most of the compounds demonstrated a poor ability to inhibit growth in tumor cell lines and did not interfere with microtubule polymerization. To analyze and compare the structure–activity relationship of compounds **2a** and **2b** with compound **1**, we hypothesized that an *ortho* substituent, such as an amino group, on the phenyl ring is essential for the formation of hydrogen bonding with the amino acids 179-Thr and 181-Val of  $\alpha$ -tubulin and the biological activity based on our ligand-docking experiments. In this study, we designed a series of 1-aryl-6-(3,4,5-trimethoxyphenyl)-3(*Z*)-hexen-1,5-diyne (**3–12**) that contain two vital components: a trimethoxyphenyl ring that could sit in the pocket of  $\beta$ -tubulin and the other aryl group bearing an *ortho* substituent that could strengthen the molecular interactions with the amino acids of  $\alpha$ -tubulin. The biological activity of these compounds was explored both *in vitro*, and the most active compound was tested in an animal model (Fig. 1).

## 2. Results and discussion

### 2.1. Chemistry

The synthesis of compounds **3–12** is shown in Scheme 1 and the yields are summarized in Table 1. 1-Chloro-4-trimethylsilyl-1(*Z*)-buten-3-yne (**13**) [10] was coupled with 3,4,5-trimethoxyphenylethyne (**14**) under Sonogashira coupling reaction conditions to give **15** with a yield of 85%. Compound **15** was then coupled with various aryl iodides **16a–i** using Pd(PPh<sub>3</sub>)<sub>4</sub> as the catalyst in the presence of K<sub>2</sub>CO<sub>3</sub> in MeOH, giving **3–9** and **11,12** with yields of 48–79%. The nitro group of **9** was reduced to an amino group using SnCl<sub>2</sub> to give **10** with a yield of 36%.

### 2.2. Biological assay results

#### 2.2.1. Cytotoxicity activities, cell cycle analysis and electrophoresis

Compounds **3–12** were tested on a panel of human cancer cell lines, including non-small-cell lung adenocarcinoma (A549), stomach adenocarcinoma (AGS), prostate cancer (PC-3), breast carcinoma (BT483), cervical epithelioid carcinoma (Hela), oral squamous cell carcinoma (SAS), hepatoma (SK Hep-1), and esophageal squamous cell carcinoma (CE81T). The IC<sub>50</sub> in each cell line

and the structure of each compound are summarized in Table 2. Compounds **5**, **6**, and **8** displayed a broad spectrum of growth inhibition against most of the cancer cell lines. Compounds **7**, **11** and **12** were inactive against the tested cell lines. Comparing the IC<sub>50</sub> of the novel compounds **3–12** with the previously designed compound **1**, compounds **4**, **5**, **6**, **8** and **9** demonstrated higher potency than compound **1**. The results support our hypothesis that two vital factors, the presence of the trimethoxyphenyl ring and an aryl group bearing an only *ortho* substituent, are essential for the biological activity of these compounds. Although the cytotoxicity of several compounds was not as potent as colchicine, compounds **5** and **8** demonstrated stronger cytotoxic activity than colchicine in BT483, HeLa and SK Hep-1 cell lines. Comparing the structure–activity relationship of compounds **5** and **12**, compound **12** had an extra methoxyl group at the *para* position of the phenyl ring, which did not contribute to its cytotoxic activity. A similar phenomenon was also observed in compounds **6** and **7**. Replacing an oxygen atom of the methoxy group of compound **5** to produce **11** decreased the IC<sub>50</sub> activity.

Because compound **8** demonstrated the highest level of activity among these synthetic enediynes, its detailed mechanism of action was investigated in the BT483 cancer cell line. BT483 cells were treated with 0.2  $\mu$ M of compound **8** for 12 h and 24 h, and the cell cycle distribution was analyzed by flow cytometry. As shown in Fig. 2A, compound **8** significantly arrested the cell cycle in the G2/M phase at 12 h post-treatment. A significant accumulation of sub-G1 cells was observed when the cells were treated with compound **8** for 24 h, suggesting that apoptosis may occur after treatment.

To confirm the occurrence of apoptosis induced by compound **8**, BT483 cells were treated with compound **8** at different concentrations for 24 h, and the cell lysate was subjected to Western blot analysis. Treatment with irinotecan was used as a positive control for apoptosis and DNA damage events. As shown in Fig. 2B, treatment with compound **8** at a 1  $\mu$ M concentration for 24 h was sufficient to induce Caspase-3 and poly (ADP-ribose) polymerase (PARP) cleavage, the early stages of apoptosis. In contrast, we found that the histone H2A variant H2AX was phosphorylated at Ser139 in response to DNA double-strand breaks after compound **8** treatment. These results indicated that compound **8** triggered a DNA damage response, consequently leading to cell apoptosis.

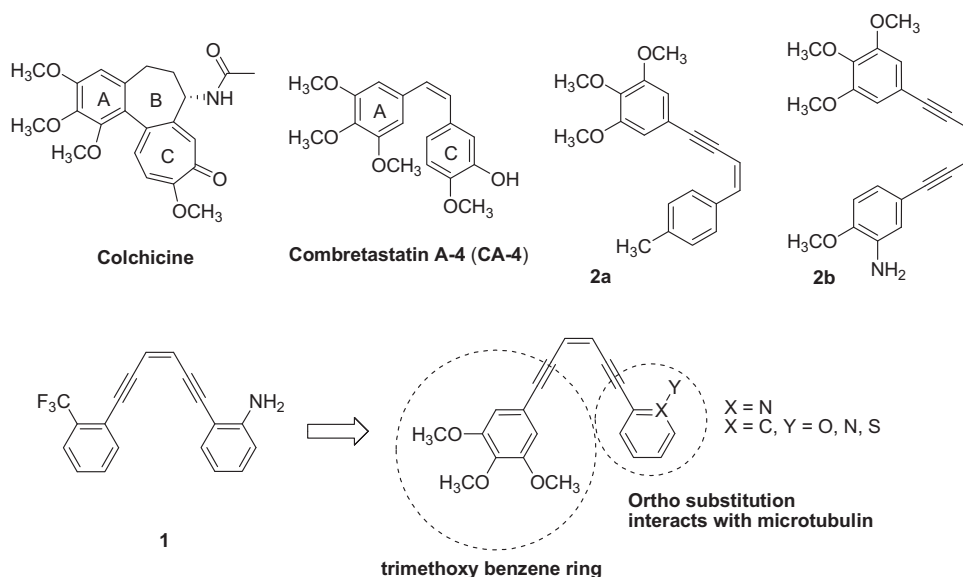
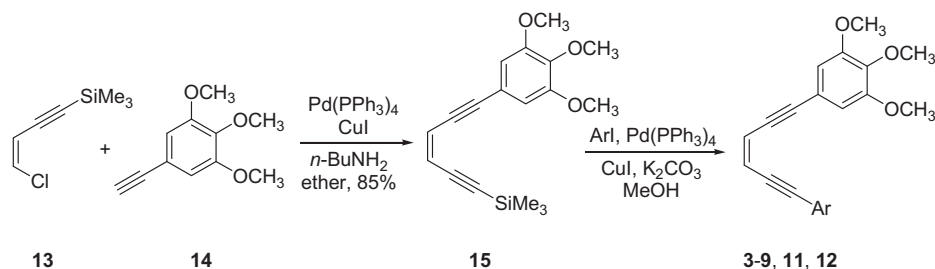


Fig. 1. Comparison and design of new antitubulin agents.



Scheme 1.

### 2.2.2. Microtubule depolymerization assay

The previously reported lead compound 2-(6-(2-trifluoromethylphenyl)-3(Z)-(hexen-1,5-diynyl)aniline (**1**) is known to destabilize microtubules. It displays significant microtubule-depolymerizing activity at a concentration of 3.6  $\mu\text{M}$ . To investigate the effects of compound **8** on microtubule polymerization, a microtubule depolymerization assay was carried out. Our data show that a brief exposure of BT483 cells to compound **8** was sufficient to produce sustained depolymerization of the microtubules at a low concentration of 1  $\mu\text{M}$  (Fig. 2C). These results suggest that the loss of microtubule function in compound **8**-treated cells at interphase may block these cells from progressing to mitosis (Fig. 2A).

### 2.2.3. Xenographic studies

The inhibitory function of compound **8** on tumor growth was evaluated in a nude mouse xenograft model. We first injected  $5 \times 10^6$  BT483 cells into nude mice subcutaneously. After the tumor grew to an appropriate size, 20 mg/kg of compound **8** or vehicle only was intraperitoneally (i.p.) injected daily for 2 weeks, and the tumor size was measured every 3 days. As shown in Fig. 3, 20 mg/kg of compound **8** dramatically diminished tumor growth compared to the tumor volume of vehicle-treated mice. These results indicated that compound **8** exhibits anti-tumor activity and may be used as an anti-breast cancer agent in future pre-clinical trials.

### 2.2.4. Molecular modeling

We performed docking experiments using the LigandFit program to investigate the binding of these synthetic compounds. A molecular model of colchicines (gray pattern) was fit to an X-ray structure of colchicines (gold) as a positive control, as shown in Fig. 4A. We previously hypothesized that compound **1** binds to  $\alpha$ - and  $\beta$ -tubulin in the same manner as colchicine [11]. The trifluoromethylphenyl group of **1** sits in the pocket of  $\beta$ -tubulin in a similar manner as the trimethoxyphenyl subunit of colchicine and the amino group of compound **1**, forming hydrogen bonds with Thr179 of  $\alpha$ -tubulin, as shown in Fig. 4B. With regard to compounds **6** and **8**, the trimethoxyphenyl rings of compounds **6** and **8** are in the same orientation as the trimethoxyphenyl subunit of

colchicine, which fits better than compound **1**. On the other side, the amino group of compound **6** and the nitrogen atom of compound **8** hydrogen bond with Thr179 of  $\alpha$ -tubulin, as shown in Fig. 4D and E. In short, these finding could explain why the trimethoxyphenyl ring and *ortho* substitution of enediyne serve as vital factors for the observed bioactivity (For interpretation of the references to color in this paragraph, the reader is referred to the web version of this article.).

## 3. Conclusion

We have successfully designed a series of novel enediyne-containing compounds, 1-aryl-6-(3,4,5-trimethoxyphenyl)-3(Z)-hexen-1,5-diynes **3–12**, based on our ligand-docking experiment results and found that these compounds show significant growth inhibition against various human cancer cell lines. After a detailed investigation of the biological activities and bio-mechanisms of these novel synthetic enediynes, we have reached several conclusions: (1) as demonstrated in the structure–activity relationship study, the cytotoxicity of compound **6** is better than compound **1**, suggesting the significance of the trimethoxyphenyl ring; (2) the addition of any substituent to the phenyl ring and substitution at the *ortho* position would reduce the potency of cytotoxicity, as evidenced by the activities of compounds **7**, **10** and **12**; (3) atoms at the *ortho* position that can form strong hydrogen bonds with the amino acids in  $\alpha$ -tubulin are vital for biological activity, as demonstrated by the activities of compounds **6** and **8**; (4) according to the results from the cell cycle distribution and Western blot analyses, compound **8** leads to a massive accumulation of cancer cells in the G2/M phase after 12 h of treatment and induces apoptosis via the activation of Caspase-3 after 24 h of treatment; (5) as demonstrated by the microtubule depolymerization assay, compound **8** can interfere with the polymerization of microtubules at 1  $\mu\text{M}$ ; (6) xenographic studies indicated that compound **8** efficiently reduced tumor sizes in BT483 tumor-bearing mice; and (7) molecular modeling studies further implicated the significance of a trimethoxyphenyl ring and *ortho* substitution at the other aryl group of the enediynes.

This study reveals a new potent antitumor agent, compound **8**, for further development as a new anticancer drug. We also believe that the information disclosed in this paper will significantly help in the development of new anticancer drugs.

## 4. Experimental section

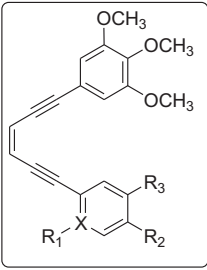
### 4.1. Cell lines and culture conditions

All cell lines were purchased from the Bioresource Collection and Research Center (Hsinchu, Taiwan). Each cell line was maintained in standard medium and grown as a monolayer in Dulbecco's modified Eagle's medium (DMEM) containing 10% fetal bovine

**Table 1**  
Chemical yields of compounds **3–9**, **11** and **12**.

Entry	Arl	Products/yields (%)
1	<b>16a</b> , Ar = 2-nitrophenyl	3/58
2	<b>16b</b> , Ar = 2-cyanophenyl	4/77
3	<b>16c</b> , Ar = 2-anisyl	5/72
4	<b>16d</b> , Ar = 2-anilinylyl	6/69
5	<b>16e</b> , Ar = 2-amino-5-trifluoromethylphenyl	7/78
6	<b>16f</b> , Ar = 2-pyridinyl	8/79
7	<b>16g</b> , Ar = 2-nitro-4-methoxyphenyl	9/48
8	<b>16h</b> , Ar = 2-thioanisyl	11/65
9	<b>16i</b> , Ar = 2,4-dimethoxyphenyl	12/49

**Table 2**  
Growth inhibition (IC<sub>50</sub>, μM) of human cancer cell lines by compounds **1**–**12**.

Compounds	Cell line <sup>a</sup>								
	A549	AGS	PC-3	BT483	HeLa	SAS	SK Hep-1	CE81T	
	Colchicine	0.07	0.05	0.06	1.45	0.66	3.50	0.78	1.78
<b>1</b>		6.57	8.24	8.26	8.56	5.49	5.83	6.68	2.91
<b>3</b> (R <sub>1</sub> = NO <sub>2</sub> , R <sub>2</sub> = H, R <sub>3</sub> = H, X = C)		5.71	4.66	4.56	4.24	1.89	1.37	1.34	6.91
<b>4</b> (R <sub>1</sub> = CN, R <sub>2</sub> = H, R <sub>3</sub> = H, X = C)		0.79	4.56	8.68	10.52	1.07	10.60	1.20	6.39
<b>5</b> (R <sub>1</sub> = OCH <sub>3</sub> , R <sub>2</sub> = H, R <sub>3</sub> = H, X = C)		0.52	0.78	0.62	1.23	0.57	9.88	0.34	6.95
<b>6</b> (R <sub>1</sub> = NH <sub>2</sub> , R <sub>2</sub> = H, R <sub>3</sub> = H, X = C)		0.57	0.98	0.73	1.98	0.64	4.53	0.20	8.98
<b>7</b> (R <sub>1</sub> = NH <sub>2</sub> , R <sub>2</sub> = H, R <sub>3</sub> = CF <sub>3</sub> , X = C)		12.41	NA	NA	21.23	24.76	15.77	28.26	21.00
<b>8</b> (R <sub>1</sub> = none, R <sub>2</sub> = H, R <sub>3</sub> = H, X = N)		3.99	0.13	0.51	0.86	0.39	1.16	0.43	6.87
<b>9</b> (R <sub>1</sub> = NO <sub>2</sub> , R <sub>2</sub> = OCH <sub>3</sub> , R <sub>3</sub> = H, X = C)		5.95	2.78	3.79	4.53	2.26	0.65	4.28	6.32
<b>10</b> (R <sub>1</sub> = NH <sub>2</sub> , R <sub>2</sub> = OCH <sub>3</sub> , R <sub>3</sub> = H, X = C)		6.42	5.75	11.67	9.56	5.00	12.28	5.23	29.97
<b>11</b> (R <sub>1</sub> = SCH <sub>3</sub> , R <sub>2</sub> = H, R <sub>3</sub> = H, X = C)		11.66	9.53	17.39	15.22	15.87	12.81	13.27	13.91
<b>12</b> (R <sub>1</sub> = OCH <sub>3</sub> , R <sub>2</sub> = OCH <sub>3</sub> , R <sub>3</sub> = H, X = C)		NA	NA	22.93	NA	12.77	NA	14.39	17.43

NA = not available.

<sup>a</sup> A549 (non-small-cell lung cancer); AGS (human stomach adenocarcinoma); PC-3 (prostate cancer); BT483 (breast carcinomas); HeLa (human cervical epithelioid carcinoma); SAS (oral squamous cell carcinoma); SK Hep (hepatocellular carcinoma); CE81T (esophageal carcinoma).

serum, 2 mM glutamine, 100 units/ml penicillin, and 100 g/ml streptomycin. Cultures were maintained at 37 °C with 5% CO<sub>2</sub> in a humidified atmosphere.

#### 4.2. Flow cytometric analysis

Apoptosis and cell cycle profiles were assessed using DNA fluorescence flow cytometry. BT-483 cells treated with DMSO or 0.2 μM compound **8** for 12 and 24 h were harvested, rinsed in PBS, resuspended, fixed in 80% ethanol, and stored at –20 °C in fixation buffer until they were ready for analysis. The pellets were suspended in 1 ml of fluorochromic solution (0.08 mg/ml PI), 0.1% Triton X-100, and 0.2 mg/ml RNase A in 1 × PBS at room temperature in the dark for 30 min. The DNA content was analyzed using a flow cytometer (FACScan; Becton Dickinson, Mountain View, CA) and CellQuest software (Becton Dickinson).

#### 4.3. Microtubule depolymerization assay

BT483 cells were maintained at 37 °C in a humidified atmosphere containing 5% CO<sub>2</sub>. To depolymerize microtubules, cells were incubated at 4 °C for 4 h. To study the effect of compound **8** on microtubule polymerization, the cells were pre-treated in the cold as described above and incubated at 37 °C for 6 h in culture medium supplemented with DMSO or 1 μM compound **8**. After fixation, immunofluorescence assays were performed with anti-tubulin antibody to examine the sub-cellular distribution of microtubules. The nuclei were counterstained by DAPI.

#### 4.4. Western blot

After the cells were treated with vehicle (1% DMSO) or compound **8** at various concentrations for 24 h, they were washed twice with PBS, and the reaction was terminated by adding 100 μL of lysis buffer. For Western blot analysis, 50 μg of protein was separated using electrophoresis in 15% SDS-PAGE and then transferred to a polyvinylidene fluoride membrane. After it had been incubated overnight at 4 °C in 5% nonfat milk, the membrane was washed and incubated with monoclonal primary antibodies for 2 h at room temperature. The antibodies used in this study were anti-Caspase-3, anti-PARP, anti-phospho-γ-H2AX, and anti-β-actin (Cell Signaling Technology). After the membrane was washed three more times, anti-mouse or anti-rabbit IgG (dilution 1:5000) was applied to the membranes, and the signals were detected using enhanced chemiluminescence reagents.

#### 4.5. Xenograft tumor growth

The nude mice (6–8 weeks old, male, 20–25 g body weight) were obtained from the National Laboratory Animal Center. The mice were maintained in a specific pathogen-free (SPF) environment at the Laboratory Animal Center of National Cheng-kung University. Animal care was provided in accordance with the Laboratory Animal Welfare Act, Guide for the Care and Use of Laboratory Animals, approved by the Institutional Animal Care and Use Committee of National Cheng Kung University. For the animal experiments, each mouse was subcutaneously inoculated with 1 × 10<sup>6</sup> BT483 cells in the left flank of legs using 50% matrigel. The tumor size was measured every 3 days with a caliper, and tumor volume was calculated as width (mm) × length (mm) × height (mm). Tumor nodules were allowed to grow to a volume of ~20 mm<sup>3</sup> before initiating treatment. Tumor-bearing mice were randomly assigned to two groups (*n* = 5–6 in each group). Test animals received intraperitoneal (i.p.) injections of DMSO (*n* = 5) or compound **8** (20 mg/kg/day) (*n* = 6) every day for 2 weeks. The tumor size was measured every 3 days beginning from the first day of compound **8** treatment.

#### 4.6. Molecular modeling

All molecular modeling studies were performed on an Asus personal computer with an Intel Core i7 2.67 GHz processor running Windows 7 using ChemBioOffice 2010 [13] and Discovery Studio 2.1 (DS) [14]. The receptor structure two tubulin dimers co-crystallized with a stathmin-like domain and N-deacetyl-N-(2-mercaptoacetyl)-colchicine (DAMA-colchicine) was downloaded from the PDB data bank (<http://www.rcsb.org/pdb/index.html>; PDB code: 1SA0) [15]. Compound structures were built with ChemBio3D in ChemBioOffice and minimized using the MMFF94 force field until an RMSD gradient of 0.1 kcal mol<sup>-1</sup> Å<sup>-1</sup> was reached. The partial charges were automatically calculated, and the structure was saved as a mol file. Docking simulations were carried out using the DS LigandFit docking module. The DAMA-colchicine present between chain A and chain B of the structure was used to define the binding site, which extended 3.0 Å from the boundary of the crystallized ligand. The GTP molecule situated at the edge of the binding site was included as a part of the receptor. DAMA-colchicine was manually removed from the active site before the docking experiment. The Jain scoring function [16] was used to measure the interaction energy between various ligand conformations and the receptor. The output of LigandFit docking was

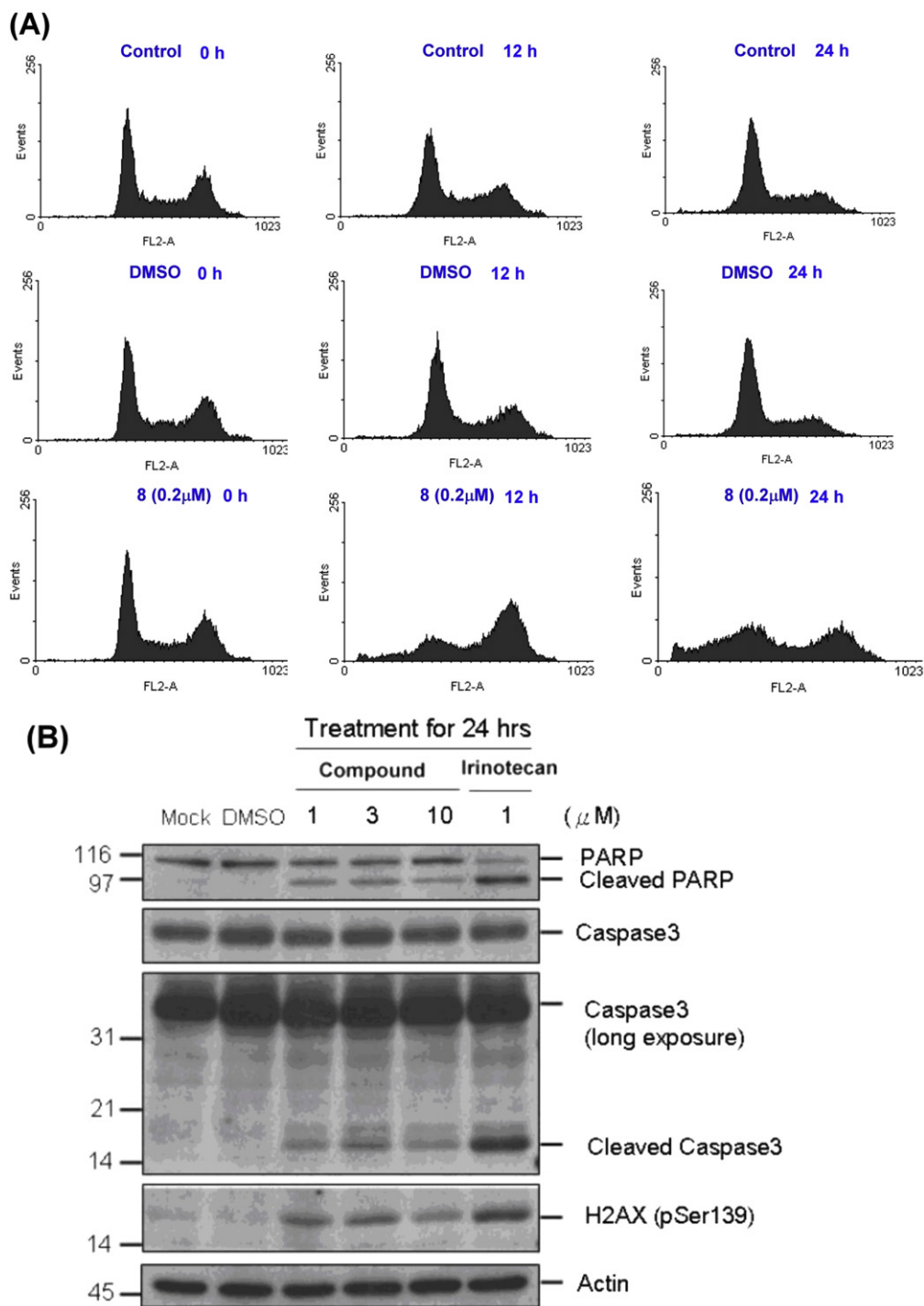


**Fig. 2.** (A) Analysis of the cancer cell cycle. (B) Expression of apoptosis-associated proteins. (C) The effect of compound **8** on microtubule depolymerization.

visualized in the DS graphics environment, and the distances of hydrogen bonds were measured between the related heavy atoms of the docked ligand and the receptor residues.

#### 4.7. Chemistry

##### 4.7.1. Synthesis of 2-(6-trimethylsilyl-3(Z)-hexen-1,5-diyne)-1,2,3-trimethoxybenzene (**15**)

To a degassed solution of **14** (12 mmol) containing CuI (3.2 mmol) and *n*-BuNH<sub>2</sub> (30 mmol) in ether (20 ml) was added

a degassed solution of compound **13** (12 mmol) containing Pd(PPh<sub>3</sub>)<sub>4</sub> (0.8 mmol) in ether (25 ml). The resulting reaction mixture was stirred at room temperature for 4 h and then quenched with saturated aqueous NH<sub>4</sub>Cl. The aqueous layer was extracted with EtOAc (30 ml  $\times$  3), and the combined organic extracts were washed with saturated aqueous Na<sub>2</sub>CO<sub>3</sub> (40 ml) and dried over anhydrous MgSO<sub>4</sub>. After filtration and removal of the solvent *in vacuo*, the residue was purified by column chromatography on a silica gel (hexane/EA = 10:1 as the eluent) to give **15** with a yield of 85% as a brown solid. Mp = 49–50 °C. <sup>1</sup>H NMR

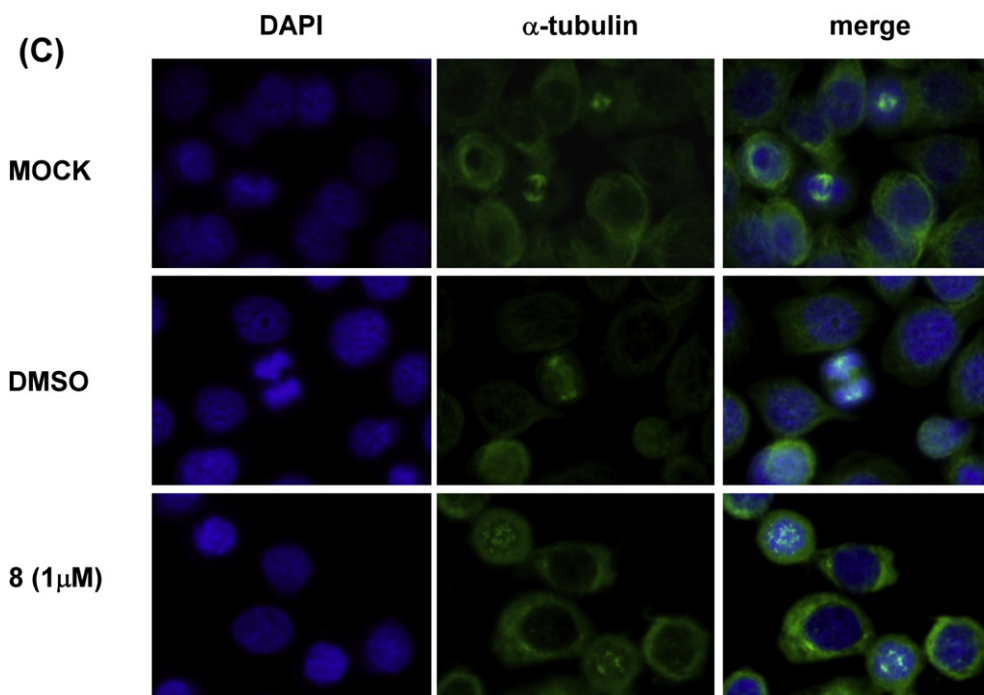


Fig. 2. (continued).

(CDCl<sub>3</sub>, 400 MHz)  $\delta$  6.71 (s, 2H), 6.05 (d, 1H,  $J = 10.8$  Hz), 5.87 (d, 1H,  $J = 10.8$  Hz), 3.86 (s, 3H), 3.84 (s, 6H), 0.24 (s, 9H). <sup>13</sup>C NMR (CDCl<sub>3</sub>, 100 MHz)  $\delta$  150.3 (2C), 139.2, 120.6, 119.1, 118.0, 108.9 (2C), 103.2, 102.3, 97.6, 86.2, 60.9, 56.1 (2C), -0.1 (3C). HRMS calcd for C<sub>18</sub>H<sub>22</sub>O<sub>3</sub>Si, Mr = 314.1338, found 314.1338. Anal. Calcd for C<sub>18</sub>H<sub>22</sub>O<sub>3</sub>Si: C, 68.75; H, 7.05. Found: C, 68.50; H, 7.06.

#### 4.7.2. General procedure for the synthesis of compounds **3–9**, **11** and **12**

To a degassed solution of 2-(6-trimethylsilyl-3(*Z*)-hexen-1,5-diynyl)-1,2,3-trimethoxybenzene (**15**) (12 mmol) containing CuI (3.2 mmol) and K<sub>2</sub>CO<sub>3</sub> (30 mmol) in MeOH (15 ml) was added a degassed solution of aryl iodides (**16a–i**) (12 mmol) containing Pd(PPh<sub>3</sub>)<sub>4</sub> (0.8 mmol) in MeOH (20 ml). The resulting reaction mixture was stirred at room temperature for 4 h. The solvent was then removed *in vacuo*. The residue was quenched with saturated aqueous NH<sub>4</sub>Cl and extracted with EtOAc (20 × 3 ml). The

combined organic extracts were washed with saturated aqueous Na<sub>2</sub>CO<sub>3</sub> (40 ml) and dried over anhydrous MgSO<sub>4</sub>. After filtration and removal of the solvent *in vacuo*, the residue was purified by column chromatography on a silica gel to produce the desired products.

4.7.2.1. 2-(6-(2-Nitrophenyl)-3(*Z*)-hexen-1,5-diynyl)-1,2,3-trimethoxybenzene (**3**). This compound was obtained at a 58% yield as a brown solid using hexane/EA (3:1) as an eluent using the general procedure. Mp = 95–96 °C. <sup>1</sup>H NMR (CDCl<sub>3</sub>, 400 MHz)  $\delta$  8.09 (dd, 1H,  $J = 8.4, 1.6$  Hz), 7.69 (dd, 1H,  $J = 7.6, 1.6$  Hz), 7.57 (td, 1H,  $J = 7.6, 1.2$  Hz), 7.47 (td, 1H,  $J = 7.6, 1.6$  Hz), 6.90 (s, 2H), 6.21 (d, 1H,  $J = 10.8$  Hz), 6.12 (d, 1H,  $J = 10.8$  Hz), 3.88 (s, 3H), 3.87 (s, 6H). <sup>13</sup>C NMR (CDCl<sub>3</sub>, 100 MHz)  $\delta$  153.0 (2C), 149.1, 139.3, 135.0, 132.8, 128.8, 124.7, 121.7, 118.7, 117.8, 117.7, 109.3 (2C), 99.2, 94.7, 92.2, 86.1, 60.9, 56.2 (2C). HRMS calcd for C<sub>21</sub>H<sub>17</sub>NO<sub>5</sub>, Mr = 363.1107, found 363.1111. Anal. Calcd for C<sub>21</sub>H<sub>17</sub>NO<sub>5</sub>: C, 69.41; H, 4.72; N, 3.85. Found: C, 68.99; H, 4.78; N, 3.35.

4.7.2.2. 2-(6-(2-Cyanophenyl)-3(*Z*)-hexen-1,5-diynyl)-1,2,3-trimethoxybenzene (**4**). This compound was obtained at 77% yield as a brown solid using hexane/EA (3:1) as the eluent using the general procedure. Mp = 64–65 °C. <sup>1</sup>H NMR (CDCl<sub>3</sub>, 400 MHz)  $\delta$  7.67 (dd, 1H,  $J = 7.2, 0.8$  Hz), 7.62 (dd, 1H,  $J = 8.0, 0.8$  Hz), 7.54 (td, 1H,  $J = 7.6, 1.6$  Hz), 7.42 (td, 1H,  $J = 7.6, 1.2$  Hz), 6.83 (s, 2H), 6.21 (d, 1H,  $J = 11.2$  Hz), 6.13 (d, 1H,  $J = 10.8$  Hz), 3.87 (s, 3H), 3.86 (s, 6H). <sup>13</sup>C NMR (CDCl<sub>3</sub>, 100 MHz)  $\delta$  153.0 (2C), 132.7, 132.6, 132.2, 128.6, 127.0, 121.5, 121.5, 117.8, 117.5, 117.3, 114.9, 109.3 (2C), 99.1, 93.2, 92.7, 86.0, 60.9, 56.2 (2C). HRMS calcd for C<sub>22</sub>H<sub>17</sub>NO<sub>3</sub>, Mr = 343.1208, found 343.1200. HPLC analysis: 96.48%.

4.7.2.3. 2-(6-(2-Anisyl)-3(*Z*)-hexen-1,5-diynyl)-1,2,3-trimethoxybenzene (**5**). This compound was obtained at 72% yield as a brown solid using hexane/EA (3:1) as the eluent using the general procedure. Mp = 66–67 °C. <sup>1</sup>H NMR (CDCl<sub>3</sub>, 400 MHz)  $\delta$  7.51 (dd, 1H,  $J = 7.6, 1.6$  Hz), 7.31 (td, 1H,  $J = 7.6, 1.6$  Hz), 6.92–6.88

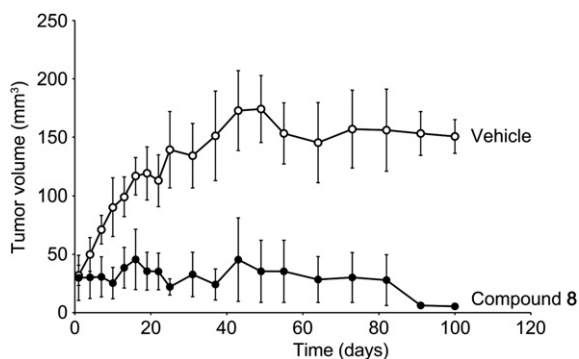
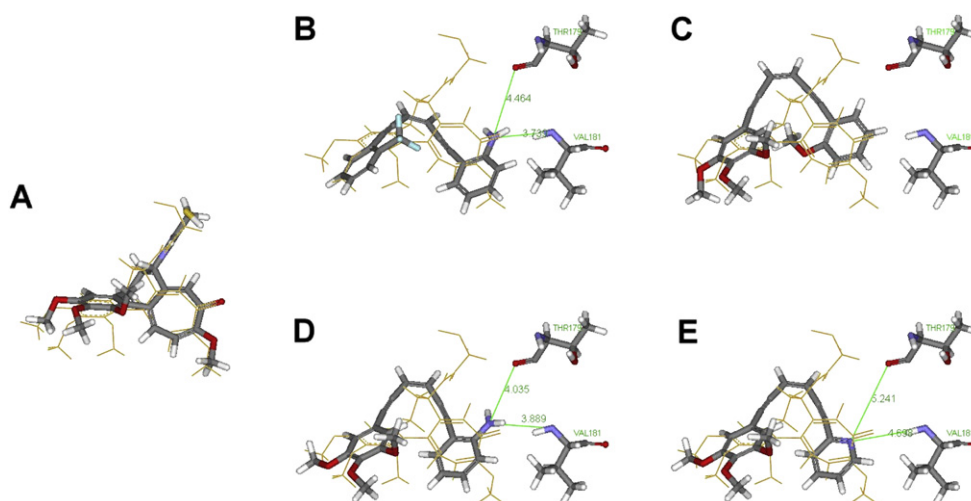


Fig. 3. Inhibitory effect of compound **8** against BT483 cell-derived tumors in nude mice. BT-483 cells were subcutaneously injected into nude mice. The tumor-bearing mice were intraperitoneally injected with either the vehicle ( $n = 5$ ) or 20 mg/kg/day of compound **8** ( $n = 6$ ) for 2 weeks. The tumor volume was measured and calculated. The data were presented as the mean  $\pm$  SEM for each group.



**Fig. 4.** Molecular modeling: (A) X-ray structure of colchicine (gold) and molecular model of colchicine (gray pattern). (B) X-ray structure of colchicine (gold) and compound **2** (gray pattern). (C) X-ray structure of colchicine (gold) and compound **5** (gray pattern). (D) X-ray structure of colchicine (gold) and compound **6** (gray pattern). (E) X-ray structure of colchicine (gold) and compound **8** (gray pattern) (For interpretation of the references to color in this figure legend, the reader is referred to the web version of this article.)

(m, 2H), 6.75 (s, 2H), 6.16 (d, 1H,  $J = 10.4$  Hz), 6.06 (d, 1H,  $J = 10.8$  Hz), 3.86 (s, 3H), 3.84 (s, 6H), 3.82 (s, 3H).  $^{13}\text{C}$  NMR ( $\text{CDCl}_3$ , 100 MHz)  $\delta$  160.0, 153.0 (2C), 139.0, 133.6, 130.2, 120.4, 119.8, 118.9, 118.2, 112.4, 110.9, 108.9 (2C), 97.5, 94.0, 91.5, 86.7, 60.9, 56.1 (2C), 55.9. HRMS calcd for  $\text{C}_{22}\text{H}_{20}\text{O}_4$ , Mr = 348.1362, found 348.1362. Anal. Calcd for  $\text{C}_{22}\text{H}_{20}\text{O}_4$ : C, 75.84; H, 5.79. Found: C, 75.43; H, 6.04.

**4.7.2.4. 2-(6-(2-Aniliny)-3(Z)-hexen-1,5-diny)-1,2,3-trimethoxybenzene (6).** This compound was obtained at 69% yield as a brown solid using hexane/EA (5:1) as the eluent using the general procedure. Mp = 132–133 °C.  $^1\text{H}$  NMR ( $\text{CDCl}_3$ , 400 MHz)  $\delta$  7.33 (dd, 1H,  $J = 8.0, 1.6$  Hz), 7.13 (td, 1H,  $J = 8.0, 1.6$  Hz), 6.75 (s, 2H), 6.70–6.65 (m, 2H), 6.17 (d, 1H,  $J = 10.8$  Hz), 6.08 (d, 1H,  $J = 10.8$  Hz), 4.36 (bs, 2H), 3.87 (s, 3H), 3.84 (s, 6H).  $^{13}\text{C}$  NMR ( $\text{CDCl}_3$ , 100 MHz)  $\delta$  153.0 (2C), 148.2, 139.1, 131.9, 130.2, 119.6, 118.1, 117.8, 117.7, 114.1, 109.2 (2C), 107.3, 97.2, 94.4, 93.2, 87.0, 60.9, 56.1 (2C). Anal. Calcd for  $\text{C}_{21}\text{H}_{19}\text{NO}_3$ : C, 75.66; H, 5.74; N, 4.2. Found: C, 75.66; H, 5.43; N, 3.9.

**4.7.2.5. 2-(6-(2-Amino-5-trifluoromethylphenyl)-3(Z)-hexen-1,5-diny)-1,2,3-trimethoxybenzene (7).** This compound was obtained at 78% yield as a brown solid using hexane/EA (5:1) as the eluent using the general procedure. Mp = 131–132 °C.  $^1\text{H}$  NMR ( $\text{CDCl}_3$ , 400 MHz)  $\delta$  7.57 (d, 1H,  $J = 2.0$  Hz), 7.34 (dd, 1H,  $J = 8.8, 2.4$  Hz), 6.73 (s, 2H), 6.72–6.70 (m, 1H), 6.17 (d, 1H,  $J = 10.8$  Hz), 6.13 (d, 1H,  $J = 10.8$  Hz), 4.68 (br s, 2H), 3.88 (s, 3H), 3.83 (s, 6H).  $^{13}\text{C}$  NMR ( $\text{CDCl}_3$ , 100 MHz)  $\delta$  153.1, 150.4 (2C), 139.3, 127.0, 125.6, 122.9, 119.8, 119.2, 119.0, 117.5, 113.5, 109.2 (2C), 106.9, 97.6, 93.9, 92.6, 86.7, 60.9, 56.1 (2C). HRMS calcd for  $\text{C}_{22}\text{H}_{18}\text{F}_3\text{NO}_3$ , Mr = 401.1239, found 401.1245. Anal. Calcd for  $\text{C}_{22}\text{H}_{18}\text{F}_3\text{NO}_3$ : C, 65.83; H, 4.52; N, 3.49. Found: C, 65.2; H, 4.35; N, 3.08.

**4.7.2.6. 2-(6-(2-Pyridinyl)-3(Z)-hexen-1,5-diny)-1,2,3-trimethoxybenzene (8).** This compound was obtained at 79% yield as a brown oil using hexane/EA (3:1) as the eluent using the general procedure.  $^1\text{H}$  NMR ( $\text{CDCl}_3$ , 400 MHz)  $\delta$  8.58 (ddd, 1H,  $J = 4.8, 1.6, 0.8$  Hz), 7.64 (td, 1H,  $J = 8.0, 2.0$  Hz), 7.50 (dt, 1H,  $J = 8.0, 0.8$  Hz), 7.23 (ddd, 1H,  $J = 7.6, 4.8, 1.2$  Hz), 6.78 (s, 2H), 6.17 (d, 1H,  $J = 10.8$  Hz), 6.09 (d, 1H,  $J = 10.8$  Hz), 3.85 (s, 3H), 3.83 (s, 6H).  $^{13}\text{C}$  NMR ( $\text{CDCl}_3$ , 100 MHz)  $\delta$  153.0, 150.1 (2C), 143.3, 135.9, 127.3, 127.3, 122.9, 121.4, 118.5, 117.9, 109.0 (2C), 98.6, 96.1, 86.8, 86.4, 60.9, 56.0 (2C). HRMS calcd for  $\text{C}_{20}\text{H}_{17}\text{NO}_3$ , Mr = 319.1208, found 319.1212. HPLC analysis: 99.90%.

**4.7.2.7. 2-(6-(4-Methoxy-2-nitrophenyl)-3(Z)-hexen-1,5-diny)-1,2,3-trimethoxybenzene (9).** This compound was obtained at 48% yield as a brown solid using hexane/EA (5:1) as the eluent using the general procedure. Mp = 97–98 °C.  $^1\text{H}$  NMR ( $\text{CDCl}_3$ , 400 MHz)  $\delta$  7.59–7.57 (m, 2H), 7.10 (dd, 1H,  $J = 8.8, 2.8$  Hz), 6.89 (s, 2H), 6.15 (d, 1H,  $J = 10.8$  Hz), 6.09 (d, 1H,  $J = 10.8$  Hz), 3.89 (s, 3H), 3.87 (s, 6H), 3.86 (s, 3H).  $^{13}\text{C}$  NMR ( $\text{CDCl}_3$ , 100 MHz)  $\delta$  159.7, 153.0 (2C), 149.9, 139.1, 135.9, 120.6, 119.9, 118.1, 117.8, 110.7, 109.3, 109.2 (2C), 98.7, 93.0, 92.5, 86.2, 60.9, 56.1 (2C), 55.9. HRMS calcd for  $\text{C}_{22}\text{H}_{19}\text{NO}_6$ , Mr = 393.1212, found 393.1210. HPLC analysis: 99.87%.

**4.7.2.8. 2-(6-(2-Amino-4-methoxyphenyl)-3(Z)-hexen-1,5-diny)-1,2,3-trimethoxybenzene (10).** This compound was obtained at 36% yield as a brown oil using hexane/EA (1:1) as the eluent via the reduction of compound **9** in a mixture of  $\text{SnCl}_2$  (5 eq) and MeOH (10 ml).  $^1\text{H}$  NMR ( $\text{CDCl}_3$ , 400 MHz)  $\delta$  7.24 (d, 1H,  $J = 8.8$  Hz), 6.74 (s, 2H), 6.27 (dd, 1H,  $J = 8.4, 2.4$  Hz), 6.16 (d, 1H,  $J = 10.8$  Hz), 6.02 (d, 1H,  $J = 10.8$  Hz), 3.87 (s, 3H), 3.84 (s, 6H), 3.76 (s, 3H).  $^{13}\text{C}$  NMR ( $\text{CDCl}_3$ , 100 MHz)  $\delta$  161.3, 153.0 (2C), 149.8, 139.0, 133.1, 119.9, 117.9, 116.8, 109.1 (2C), 104.6, 100.3, 98.9, 96.7, 94.9, 92.5, 87.2, 60.9, 56.1 (2C), 55.1. HRMS calcd for  $\text{C}_{22}\text{H}_{21}\text{NO}_4$ , Mr = 363.1471, found 363.1472. HPLC analysis: 98.3%.

**4.7.2.9. 2-(6-(2-Thioanisyl)-3(Z)-hexen-1,5-diny)-1,2,3-trimethoxybenzene (11).** This compound was obtained at 65% yield as a brown oil using hexane/EA (3:1) as the eluent using the general procedure.  $^1\text{H}$  NMR ( $\text{CDCl}_3$ , 400 MHz)  $\delta$  7.48 (dd, 1H,  $J = 7.6, 1.2$  Hz), 7.29 (td, 1H,  $J = 7.6, 1.2$  Hz), 7.16 (d, 1H,  $J = 8.0$  Hz), 7.07 (td, 1H,  $J = 7.6, 1.2$  Hz), 6.78 (s, 2H), 6.17 (d, 1H,  $J = 10.4$  Hz), 6.11 (d, 1H,  $J = 10.8$  Hz), 3.86 (s, 3H), 3.82 (s, 6H), 2.40 (s, 3H).  $^{13}\text{C}$  NMR ( $\text{CDCl}_3$ , 100 MHz)  $\delta$  152.9 (2C), 141.8, 139.0, 132.6, 129.0, 124.2, 124.1, 121.2, 119.4, 119.1, 118.2, 109.2 (2C), 97.8, 94.6, 93.6, 86.7, 60.9, 56.1 (2C), 15.1. HRMS calcd for  $\text{C}_{22}\text{H}_{20}\text{O}_3\text{S}$ , Mr = 346.1133, found 346.1136. HPLC analysis: 99.68%.

**4.7.2.10. 2-(6-(2,4-Dimethoxyphenyl)-3(Z)-hexen-1,5-diny)-1,2,3-trimethoxybenzene (12).** This compound was obtained at 49% yield as a brown solid using hexane/EA (5:1) as the eluent using the general procedure. Mp = 77–78 °C.  $^1\text{H}$  NMR ( $\text{CDCl}_3$ , 400 MHz)  $\delta$  7.41 (d, 1H,  $J = 9.2$  Hz), 6.75 (s, 2H), 6.44–6.41 (m, 2H), 6.14 (d, 1H,  $J = 10.4$  Hz), 6.01 (d, 1H,  $J = 10.8$  Hz), 3.86 (s, 3H), 3.82 (s, 6H), 3.81 (s, 3H), 3.80 (s, 3H).  $^{13}\text{C}$  NMR ( $\text{CDCl}_3$ , 100 MHz)  $\delta$  161.6, 161.3, 153.0

(2C), 134.5, 120.2, 120.2, 118.4, 117.8, 108.9 (2C), 105.1, 104.9, 98.5, 97.1, 94.4, 90.4, 86.9, 60.9, 56.1 (2C), 55.9, 55.5. Anal. Calcd for  $C_{23}H_{22}O_5$ : C, 73.00; H, 5.86. Found: C, 72.99; H, 6.00.

## Acknowledgments

We would like to thank the National Science Council of the Republic of China for the financial support.

## Appendix A. Supplementary data

Supplementary data associated with this article can be found in the online version, at <http://dx.doi.org/10.1016/j.ejmech.2013.01.011>.

## References

- [1] E. Nogales, Structural insight into microtubule function, *Annu. Rev. Biophys. Biomol. Struct.* 30 (2001) 397–420.
- [2] M.A. Jordan, L. Wilson, Microtubules as a target for anticancer drugs, *Nat. Rev. Cancer* 4 (2004) 253–265.
- [3] C. Dumontet, M.A. Jordan, Microtubule-binding agents: a dynamic field of cancer therapeutics, *Nat. Rev. Drug Discov.* 10 (2010) 790–803.
- [4] (a) P.B. Schiff, J. Fant, S.B. Horwitz, Promotion of microtubule assembly *in vitro* by taxol, *Nature* 277 (1979) 665–667; (b) R.M. Buey, I. Barasoain, E. Jackson, A. Meyer, P. Giannakakou, I. Paterson, S. Mooberry, J.M. Andreu, J.F. Díaz, Microtubule interactions with chemically diverse stabilizing agents: thermodynamics of binding to the paclitaxel site predicts cytotoxicity, *Chem. Biol.* 12 (2005) 1269–1279.
- [5] (a) M.A. Jordan, J.A. Hadfield, N.J. Lawrence, A.T. McGown, Tubulin as a target for anticancer drugs: agents which interact with the mitotic spindle, *Med. Res. Rev.* 18 (1998) 259–296; (b) S. Lobert, B. Vulevic, J.J. Correia, Interaction of vinca alkaloids with tubulin: a comparison of vinblastine, vincristine, and vinorelbine, *Biochemistry* 35 (1996) 6806–6814.
- [6] Q. Li, H. Sham, S. Rosenberg, Antimitotic agents, *Annu. Rep. Med. Chem.* 34 (1999) 139–148.
- [7] (a) N.H. Nam, Combretastatin A-4 analogues as antimitotic antitumor agents, *Curr. Med. Chem.* 10 (2003) 1697–1722; (b) P.E. Thorpe, Vascular targeting agents as cancer therapeutics, *Clin. Cancer Res.* 10 (2004) 415–427.
- [8] (a) G.M. Tozer, C. Kanthou, C.S. Parkins, S.A. Hill, The biology of the combretastatins as tumour vascular targeting agents, *Int. J. Exp. Pathol.* 83 (2002) 21–38; (b) V.E. Prise, D.J. Honess, M.R. Stratford, J. Wilson, G.M. Tozer, The vascular response of tumor and normal tissues in the rat to the vascular targeting agent, combretastatin A-4-phosphate, at clinically relevant doses, *Int. J. Oncol.* 21 (2003) 717–726; (c) G.G. Dark, S.A. Hill, V.E. Prise, G.M. Tozer, G.R. Pettit, D.J. Chaplin, Combretastatin A-4, an agent that displays potent and selective toxicity toward tumor vasculature, *Cancer Res.* 57 (1997) 1829–1834.
- [9] I. Vitale, A. Antocchia, C. Cenciarelli, P. Crateri, S. Meschini, G. Arancia, C. Pisano, C. Tanzarella, Combretastatin (CA-4) and combretastatin derivative induce mitotic catastrophe dependent on spindle checkpoint and Caspase-3 activation in non-small cell lung cancer cells, *Apoptosis* 12 (2006) 155–166.
- [10] (a) Y.H. Lo, C.F. Lin, M.C. Hsieh, M.J. Wu, Remarkable G2/M phase arrest and apoptotic effect performed by 2-(6-aryl-3-hexen-1,5-diynyl) benzonitrile antitumor agents, *Bioorg. Med. Chem.* 12 (2004) 1047–1053; (b) C.F. Lin, Y.H. Lo, M.C. Hsieh, Y.H. Chen, J.J. Wang, M.J. Wu, Cytotoxicities, cell cycle and caspase evaluations of 1,6-diaryl-3(Z)-hexen-1,5-diynes, 2-(6-aryl-3(Z)-hexen-1,5-diynyl)anilines and their derivatives, *Bioorg. Med. Chem.* 13 (2005) 3565–3575; (c) Y.H. Lo, C.C. Lin, C.F. Lin, Y.T. Lin, T.H. Duh, Y.R. Hong, S.H. Yang, S.R. Lin, S.C. Yang, L.S. Chang, M.J. Wu, 2-(6-Aryl-3(Z)-hexen-1,5-diynyl) anilines as a new class of potent antitubulin agents, *J. Med. Chem.* 51 (2008) 2682.
- [11] Y.S. Tu, T.H. Duh, C.Y. Tseng, T.Y. Lin, Y.H. Lo, Y.L. Hu, C.H. Chen, C.M. Chien, S.H. Yang, S.R. Lin, S.C. Yang, M.J. Wu, 1-(2-((Z)-6-(2-(Trifluoromethyl)phenyl) hexa-3-en-1,5-diynyl)phenyl)-piperidin-2-one as a new potent apoptosis agent, *Bioorg. Med. Chem.* 17 (2009) 7412–7417.
- [12] O. Provot, A. Giraud, J.-F. Peyrat, M. Alami, J.-D. Brion, Synthetic approach to enyne and enediene analogues of anticancer agents, *Tetrahedron Lett.* 46 (2005) 8547–8550.
- [13] S.M. Kerwin, ChemBioOffice Ultra 2010 suite, *J. Am. Chem. Soc.* 132 (2010) 2466–2467.
- [14] Discovery Studio 2.1, Accelrys Software Inc., San Diego, CA, USA, 2008.
- [15] R.B. Ravelli, B. Gigant, P.A. Curmi, I. Jourdain, S. Lachkar, A. Sobel, M. Knossow, Insight into tubulin regulation from a complex with colchicine and a stathmin-like domain, *Nature* 428 (2004) 198–202.
- [16] A.N. Jain, J. Scoring, Noncovalent protein–ligand interactions: a continuous differentiable function tuned to compute binding affinities, *J. Comput.-Aided Mol. Des.* 10 (1996) 427–440.